Bima Journal of Science and Technology, Vol. 9(1A) Mar, 2025 ISSN: 2536-6041

DOI: 10.56892/bima.v9i1A.1236

Adsorption Experiment for Measuring the Atenolol Adsorbing Ability of Thermally Reduced Graphite Oxide

Ladan H. M. A.[1]*, Buba A. D. A.[2] and Umar M.[1]

[1a]Department of Physics, Faculty of Science, Sa'adu Zungur University, Bauchi State
[1b]CEMS group, Department of Physics, Sa'adu Zungur University, Bauchi State, Nigeria
[2]Department of Physics, Faculty of Science, University of Abuja, Abuja.

Corresponsing Author: ladansons@gmail.com; ladan@basug.edu.ng

ABSTRACT

In this study, the microscopic and spectroscopic analysis of thermally reduced graphite oxide and testing its adsorbing ability from 50 to 400 ^{0}C was conducted. The samples were characterized by X-ray fluorescence (XRF), X-ray diffraction (XRD), field emission scanning electron microscopy (FESEM), UV visible near infra-red and Fourier transforms (FTIR) spectroscopy to ascertain the crystalline nature, morphology, photo response, bonding and functional groups. The sample was tested for the removal of atenolol (ATL) in aqueous solutions by adsorption experiment. XRF analysis showed the presence of C, MgO, SiO_2, and SrO at 15.0%, 4.35%, 25.14%, and 9.73% respectively. XRD spectra showed the crystalline forms and sharp diffraction peak**.** SEM analysis revealed reflective surface and impurity sites. The study has proved that the RGO is suitable for the removal of ATL at 60% and the graphite is effective in treating water contaminated with drugs for treating cardiovascular diseases. It is of high quality and suitable for exportation as a source of foreign exchange.

Keywords: Cardiovascular diseases, Atenolol, Graphite, carbon, Adsorption

INTRODUCTION

Graphite occurs naturally in the ore form. There are several deposits of graphite in Nigeria especially in the states where flood and accumulation of debris takes place. Generally, beneficiation is performed to recover the pure graphite from its ore (Nwoke et al., 2017; RMRDC, 2019; Barma et al., 2019; Kaitano et al., 2023). There is carbon in graphite and diamonds, coal and petroleum, limestone and dolomite. Carbon atoms are hexagonally arranged in graphitic layers. It is used in conductors and is one of the raw materials in the production of batteries, solar panels, electrical appliances, electrodes, plumbing materials, chemicals, lubricants, foundry facings, drugs, polishes, cosmetics, and pencils (ACS, 2018; Kiciński et al., 2020; Sankaran et al., 2020; Dhakate et al., 2020, Kim et al., 2023). The reduced graphene oxide (RGO) is obtained by chemical or thermal reduction of the graphitic oxide. It has strong sp^2 hybridized carbon atoms, large surface areas (~2600 m^2/g), several functional groups, and higher conductivities. They are widely used in chemicals and drugs adsorption (Geim et al., 2007, Kyzas et al., 2015; Coros et al., 2020; Kiciński et al., 2020; Kim et al., 2023; Ali et al., 2024).

Cardiovascular diseases (CVDs) are disorders of the heart and blood vessels due to tobacco use, an unhealthy diet or use of alcohol (WHO, 2023). Different medications such as beta blockers, angiotensin II receptor blockers, anticoagulants, angiotensin-converting enzyme inhibitors, calcium channel blockers, anti-platelets (aspirin, acetylsalicylic acid, clopidogrel, dipyridamole, ticlopidine), digoxin, statins, and diuretics are administered. Atenolol (ATL), Betaxolol (Kerlone),

DOI: 10.56892/bima.v9i1A.1236

Bisoprolol/hydrochlorothiazide (Ziac), Bisoprolol (Zebeta), Metoprolol (Lopressor, Toprol XL), Nadolol (Corgard), Propranolol (Inderal), and Sotalol (Betapace) are specific drugs used for CVDs. Some of them are not fully metabolized by the human body system (AHA, 2023). They are mostly found in waste waters.

Researchers have identified ways of treating water contaminated with ATL by photochemical and photocatalytic degradation (Dong et al. 2015; Tammaro et al. 2017), adsorption (Kyzas et al. 2015; Jeirani et al. 2017; Coros et al. 2020), and chromatography (Tay et al., 2011). Few studies have been conducted on the removal of ATL using GO (Kyzas et al., 2015), titania/silica on glass slides (Píšťková et al. 2015); activated carbon (Jeirani et al., 2017), titanium dioxide (Tammaro et al. 2017), BiOCl facilitated (Hu et al. 2018) and reduced GO (Coros et al. 2020) while Haro et al. 2017 studied the kinetics and equilibrium situation. They all used the safe and efficient adsorption methods. None of these studies performed the characterizations and applications of the RGO of naturally occurring graphite like ANG at lower temperatures and ATL adsorption from aqueous solutions. To the best of our knowledge, no such studies using ANG from the north east have been conducted in the manner presented here.

Experimental Details

Oxidizing and Reducing ANG

The procedure for oxidizing and thermally reducing ANG was adopted from Ladan and Buba, 2021. The methods can summarized briefly as follows. In the low temperature stage, 5 g of the ANG was mixed with conc. H_2SO_4 and HNO_3 in 3:1 and was sonicated for 30 minutes before adding $KMnO_4$ (6 g) and the stirring continued under ice bath below 5 ^{0}C. The temperature of the mixture was raised to 30 ^{0}C with continuous stirring until a golden yellow colouration was formed at 80 ^{0}C. The reaction was stopped, centrifuged and watched with dilute HCl. Finally, the obtained samples were reduced between 10 ^{0}C and 100 ^{0}C respectively.

Microscopic and spectroscopic analysis of ANG

The mineralogical, structural, and chemical composition of the ANG was investigated using the X-ray fluorescence spectrometer (ARL QUANTX thermos-fisher, 9952120 UMYU). The morphological features of the samples were observed on SEM (PRO X, Phenonm 01570775, UMYU). The phase composition was identified using XRD (ARL XTRA no. 1974992086) with Cu$K_\propto$ radiation (k = 1.5406 nm). The UV VIS NIR spectra of the thermally reduced ANG oxide in solution was measured on a T80+ UV-vis spectrophotometer to determine the photo response. The nature of the functional groups were observed by Fourier transforms infrared (FTIR) spectroscopy (Nicolet i-S50) to scan the specimen from 650 to 4000 cm^{-1} at raw material research labouratory, Abuja, Nigeria.

Adsorption experiment

The adsorption studies were performed at room temperature in a 100 mL round bottom flask containing 50 mg/L of the ATL and 1.50 mg/mL RGO. The suspension was left undisturbed for 45 minutes. The samples were then filtered. Then, the UV-Vis spectra analysis was conducted using T80 spectrophotometer (Nile University, labouratory). The procedures were repeated for other samples.

RESULTS AND DISCUSSION

XRF and XRD analysis

The XRF analysis of the ANG showed the presence of C, MgO, SiO_2, and SrO at 15.0%,

DOI: 10.56892/bima.v9i1A.1236

4.35%, 25.14%, and 9.73% respectively. The XRD was used to determine the crystal structures, mineral phase, and identification of impurities. It indicates the minerals and impurities in graphite ore (Kiciński et al. 2020). The XRD patterns of the pristine ANG shows a characteristic (002) peak at 26.5˚ (2θ) corresponding to an interlayer spacing of 3.35 Å d_{hkl} (Figure 1) was calculated with the Bragg's law (Eluyemi et al. 2016; Gurzęda et al. 2019).

$$d = \frac{\lambda}{2\sin\theta} \qquad 1$$

where λ is the wavelength and hkl are miller indices

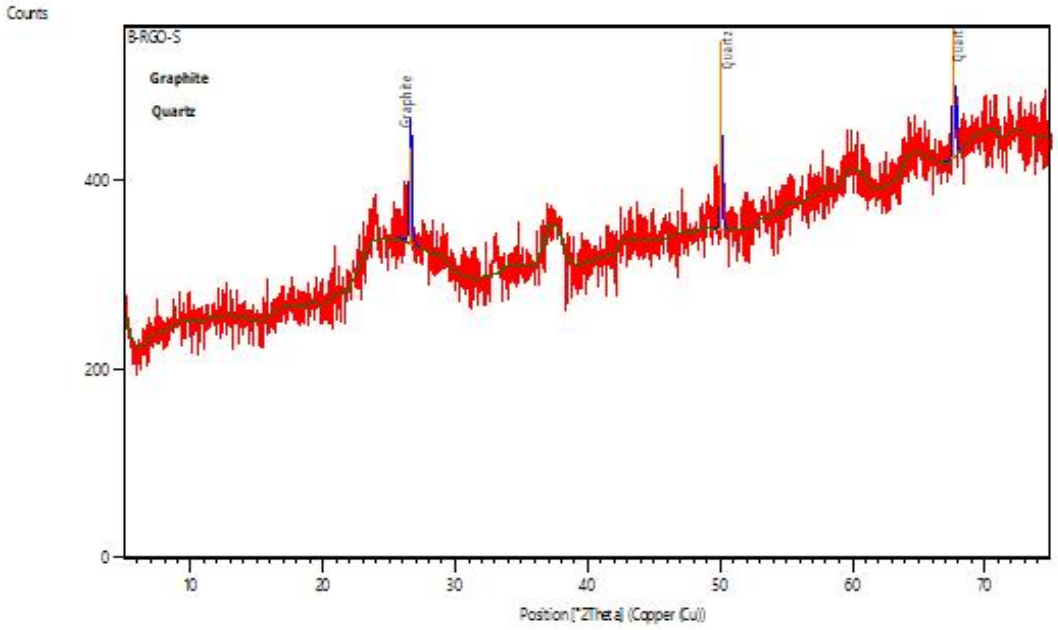

Figure 1: XRD pattern of the RGO on quartz.

SEM Analysis

The SEM analysis at magnification of 500x, 600x and 800x (Figure 2) revealed the morphological characteristics of the graphite (Gurzęda et al., 2019) samples in layers (Figure 3) with reflective surfaces when exposed to light. Mapped areas were due to foreign atoms and impurities (Mg, Sr and Si), dislocation and substitution were spotted on the graphite layer (Ladan and Buba, 2021).

Fourier Transforms Infrared Spectroscopy

Fourier Transforms Infrared (FTIR) spectroscopy of the RGO identified the bonding interactions and functional groups in the RGO. The percentage transmittance on the y axis showed how strongly light is being absorbed at each frequency while the IR wavelength in terms of the wave number cm^{-1} was indicated on the x-axis. The RGO had an aromatic (C=C), carbonyl (C=O), and epoxy (C-O-C) functional groups to some extent without COOH group due to drastic decrease in the bands associated with the oxygen-containing groups. The strong band at 2367.65 cm^{-1} due to the stretching vibrational modes of the C = O (Figure 3 and 4) disappeared upon reduction to about 1716.11.32 cm^{-1} (Paulchamy et al. 2015; Eluyemi et al. 2016; Ladan and Buba, 2021).

DOI: 10.56892/bima.v9i1A.1236

A well-ordered layered graphite oxide with high oxidation degree (Gurzęda et al. 2019).

The red shift in the UV-vis absorption spectra can be attributed to the restoration of the sp^2 hybridization of the carbon atoms in the hexagonal pattern and the increase in electron concentration. The RGO-400 sample had the higher red shift from 250 to 330 nm, it contained fewer carbonyl group and purer graphene. Due to the evaporation of the water molecule and oxygen functional groups, weight loss of RGO which occurred from 50 °C to 400 °C was noticed (Coros et al. 2020).

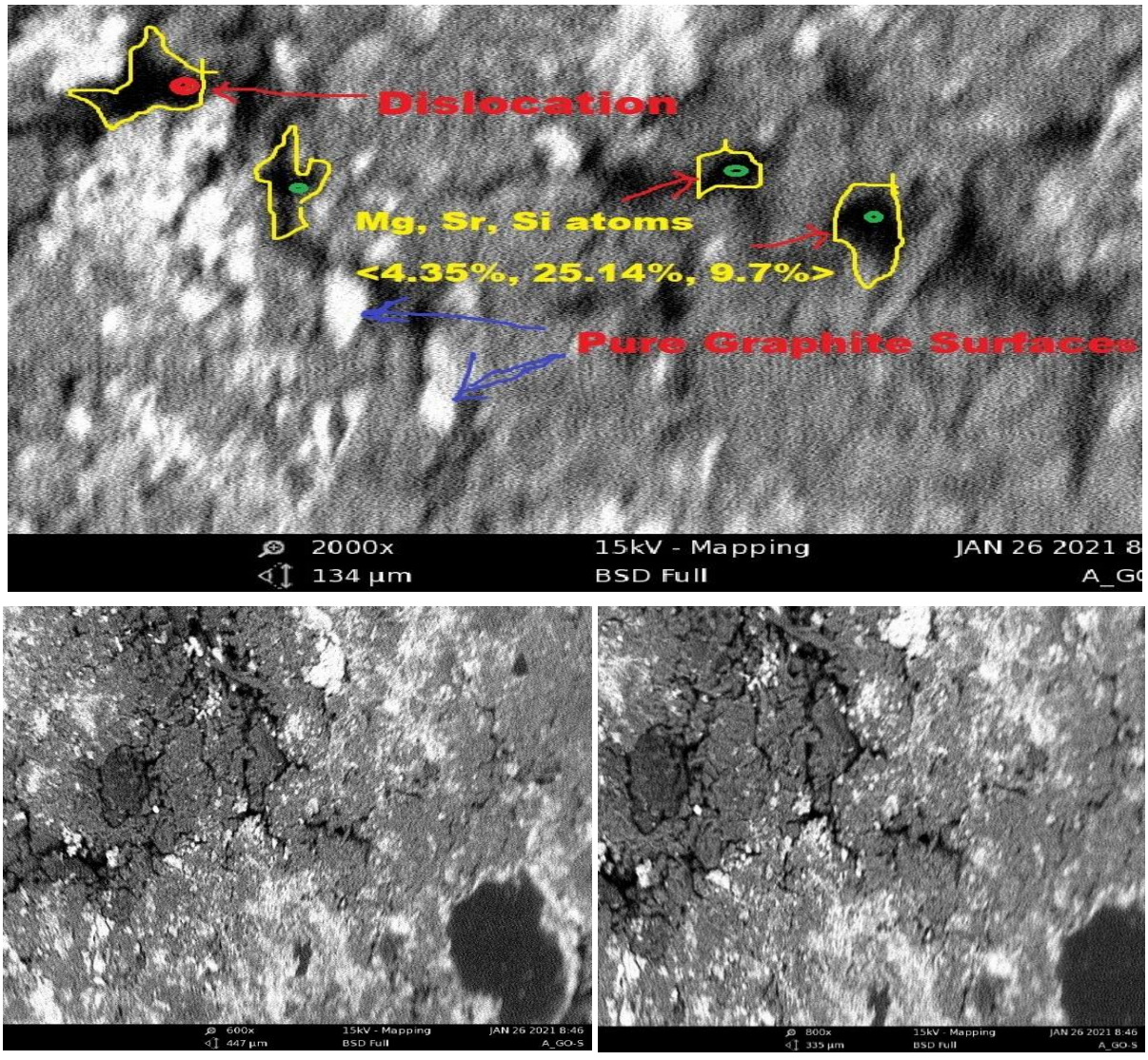

Figure 2: SEM micrograph of the graphite at magnification of (a) 500x (b) 600x (c) 800x with surface elements.

Bima Journal of Science and Technology, Vol. 9(1A) Mar, 2025 ISSN: 2536-6041

DOI: 10.56892/bima.v9i1A.1236

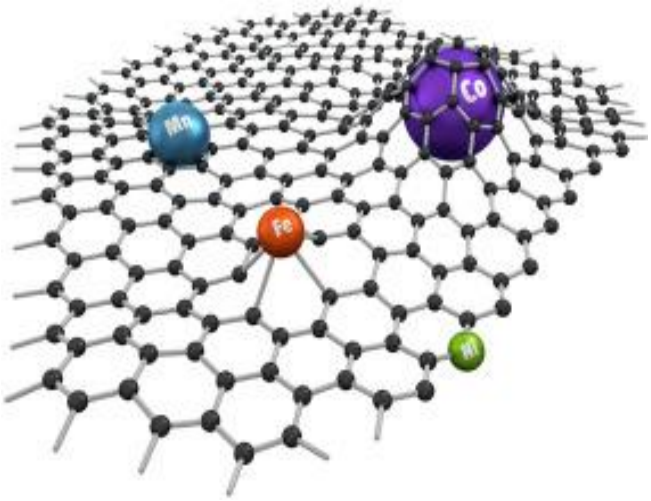

Figure 3: Typical graphite with surface elements (Kiciński et al., 2020)

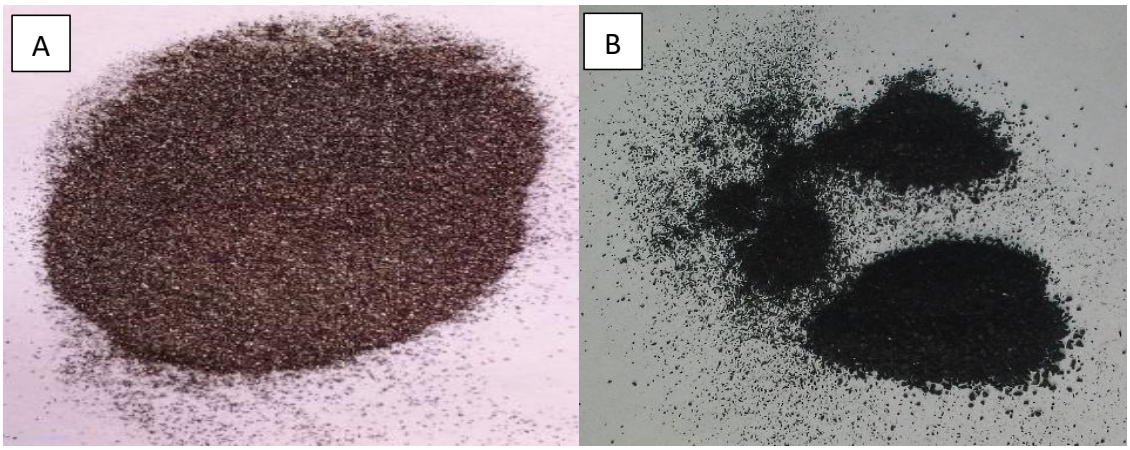

Figure 4: (a) Beneficiated ANG and (b) RGO in powdered forms

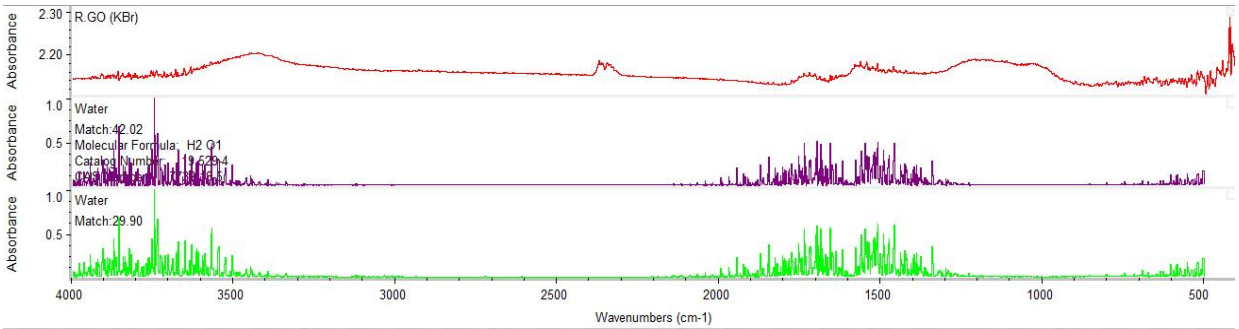

	Index	Match	Compound Name	Library Name
1	242	42.02	Water	HR Aldrich Solvents
2	59	29.90	Water	HR Specta IR Demo
3	20	26.11	URETHANE ALKYD, LINSEED OIL-RICH	Hummel Polymer Sample Library
4	4435	25.08	Silver(I) oxide - ReagentPlus(R), 99% - ATR-IR	Sigma-Aldrich ATR-IR Library (Wiley)
5	38	25.07	L-A-PHOSPHATIDYLINOSITOL	Sigma Biological Sample Library
6	54	22.43	MONOELAIDIN	Sigma Biological Sample Library
7	57	21.57	FORMANILIDE, 97%	Aldrich Condensed Phase Sample Library
8	118	21.02	PHENYTOIN IN KBR	Georgia State Crime Lab Sample Library

Figure 5: Absorbance versus wave numbers and atomic vibrations for RGO on KBr

DOI: 10.56892/bima.v9i1A.1236

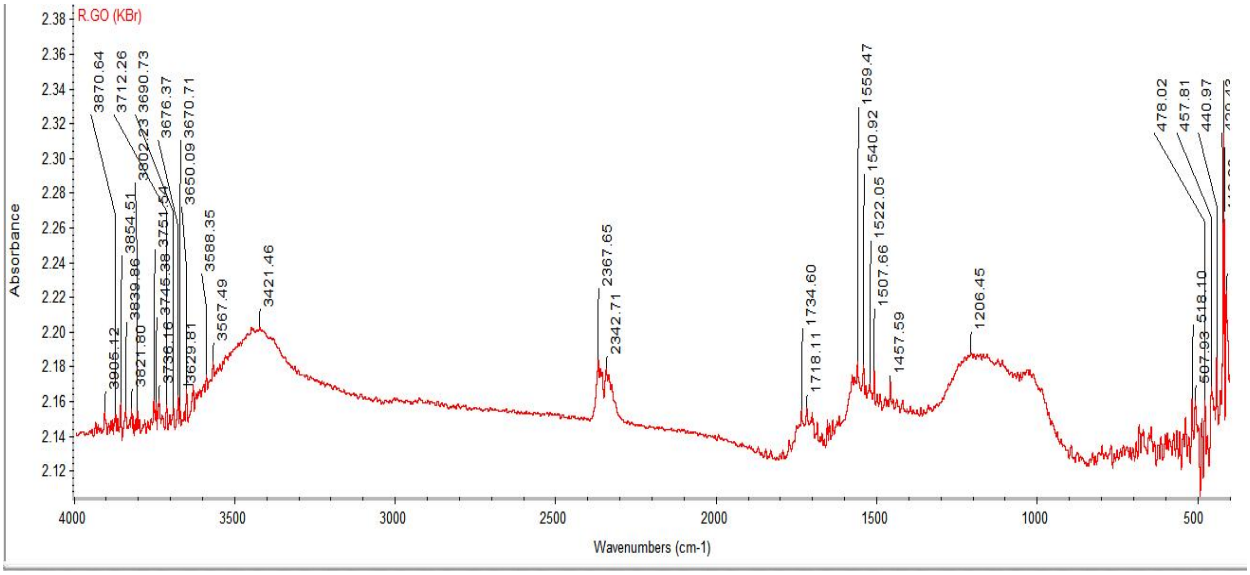

Figure 6: FTIR spectrum of RGO powder the absorbance against wave numbers

UV-visible spectra of the ANG in solution

The UV-Vis spectra of the RGO in solution behaves like a semiconductor (Fig. 6). The energy band gaps in semiconductors are closely related to the wavelength range they absorbed (table 1). It decreases with increasing absorption wavelength and vice versa (Kumar et al., 2019). UV response of the ATL-RGO showed an absorbance peak at 280 nm. For the RGO, the absorbance peak is at 600 nm. The decrease in the absorbance peak of RGO-ATL can be attributed to the formation of ATL-RGO mixture (Ladan and Buba, 2021).

Table 1: Absorbance coefficient of RGO

λ (nm)	Abs. of RGO	$\alpha = 4\pi k_B/\lambda (x\ 10^{-16})$
200	0.172	8.67
300	0.311, E_g = 4.01	5.78
400	0.252	4.35
500	0.290	3.47
600	0.315, E_g = 2.10	2.89
700	0.271	2.48
800	0.238	2.17

DOI: 10.56892/bima.v9i1A.1236

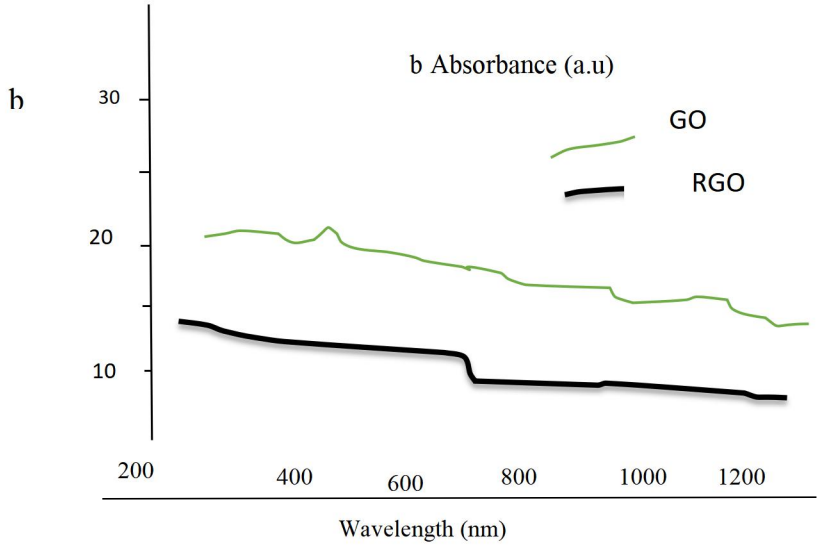

Figure 7: Absorbance versus wavelength of the GO and RGO

Removal of ATL in Aqueous Solutions

The prepared sample was used to demonstrate the removal of ATL in aqueous solutions by adsorption using the synthesized RGO (Table 2).

Table 2: Removal of ATL in aqueous solutions

Sample	T (^{0}C)	ATL ratios (mg/mL)	C_t	γ (%)
RGO	25	10	0.16	8.10
RGO	50	20	0.10	14.00
RGO	100	30	0.06	24.50
RGO	200	40	0.02	60.20
RGO	400	50	0.04	40.40

The ATL removal efficiency increases as the reduction temperature increases to the peak 200 ^{0}C (60%) proving that a well reduced graphene is not very suitable for atenolol adsorption due to the reduction process. The effect of atenolol concentration on the adsorption on RGO was determined by keeping constant the initial concentration at 1.50 mg/L. The experiments were carried out with different ATL ratios from 10 to 50 mg/mL. Since RGO contains a small amount of the functional groups, large surface areas (Paulchamy et al., 2015) and high reactivity carbon atoms to achieve chemical stability. It is applicable in water purification. The ATL removal efficiency γ can be calculated as

$$\gamma = \frac{C_i - C_t}{C_t} x\ 100 \qquad 2$$

Where C_t (mg/L) is the concentration of ATL at time t, and C_i (mg/L) is the initial concentration of ATL.

DOI: 10.56892/bima.v9i1A.1236

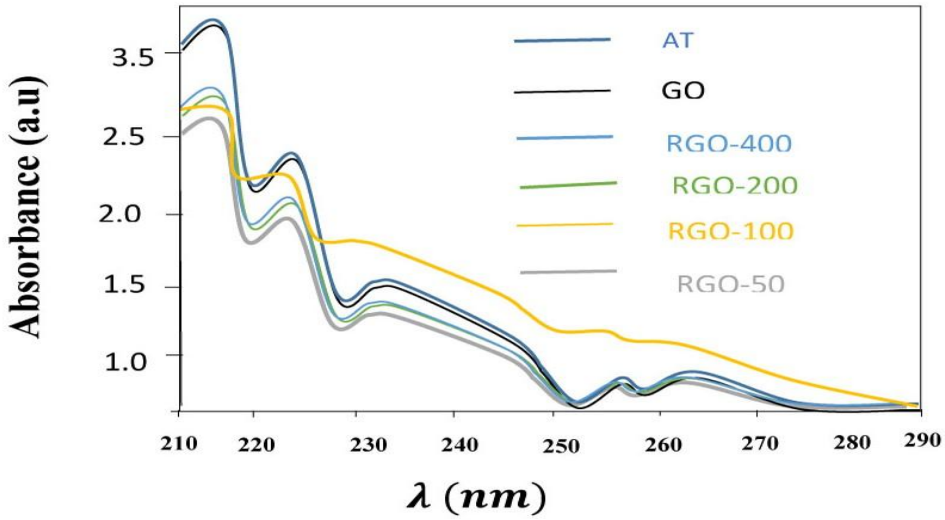

Figure 8: UV-Vis spectra of purple ATN (AT) and its removal when treated with RGO-50; RGO-100; RGO-200; and RGO-400

CONCLUSION

In the present work, the analysis of natural graphite was carried out. The SEM and XRD analysis showed that the graphite flakes were perfectly crystallized and closely packed. The RGO obtained by oxidation of the graphite is suitable for water purification and the removal of ATL in aqueous solutions. The optimum temperature has been determined to be 200°C for efficient adsorption of ATL using RGO at 60%. The study also indicated the possibility of using ANG available in abundant at low cost for industrial production. The results obtained were in line with the available statistics in the literature.

REFERENCES

1. World Health Organization WHO (2024), www.who.int/news-room/fact-sheets/detail/cardiovascular-diseases accessed January 20, 2024.
2. American Heart Association AHA (2024) accessed January 20, 2024. www.heart.org/en/health-topics/heart-attack/treatment-of-a-heart-attack/cardiac-medications,
3. Barma SD, Baskey PK, Rao DS, Sahu SN (2019) Ultrasonic-assisted flotation for enhancing the recovery of flaky graphite from low-grade graphite ore, Ultrasonics-Sonochemistry. 2019. 56:386-396.
4. Beaussart A, Mierczynska-Vasilev A, Beattie DA. Adsorption of dextrin on hydrophobic minerals. Langmuir ACS J. Surf. Colloids 2009; 25 (9):9913-9921.
5. Eluyemi MS, Eleruja MA, Adedeji AV, et al. Synthesis and Characterization of Graphene Oxide and Reduced Graphene Oxide Thin Films Deposited by Spray Pyrolysis Method. Graphene, 2016; 5:143-154.
6. Kumar A, Ratan S, Jarwal DK, Mishra AK, Kumar C, (2019) Effect of PQT-12 interface layer on the performance of PCDTBT: PCBM bulk heterojunction solar cells, Mater. Res. Express; 6:1-9
7. Patil MR, Shivakumar KS, Rudramuniyappa MV, Rao RB. Flotation studies on graphite ores of shivaganga area, Madurai district, Tamilnadu. Journal of Metallurgy and Materials Science, 2000; 42(4):233-241.

DOI: 10.56892/bima.v9i1A.1236

8. RMRDC graphite location chart www.rmrdc.gov.ng (accessed May, 5 2019)
9. Nwoke MAU, Uwadiale GGOO, Kollere MA. (1997) Flotation of low-grade Birnin Gwari and Alawa graphite, Nigeria. Mining, Metallurgy & Exploration, 14(2), 54-56
10. Ladan H.M.A and Buba A.D.A (2021) Synthesis, Characterization and Simulation of 2D Graphene for Perovskite Solar Cells, Ph.D Thesis, Department of Physics, Faculty of Science, University of Abuja, Nigeria. phyfosuofA-21/15538006/07/2021 UniAbuja www.researchgate.net/profile/Muhammed-Ladan
11. Coros, Maria; Pogacean, Florina…; Pruneanu, Stela (2020). Green synthesis, characterization and potential application of reduced graphene oxide. Physica E: LD Systems and Nanostructures, 113971 doi:10.1016/j.physe.2020.113971
12. Dong MM; Trenholm R; Rosario-Ortiz FL (2015) Photochemical degradation of atenolol, carbamazepine, meprobamate, phenytoin and primidone in wastewater effluents, J. Hazard. Mater. 282, 216-223. doi.org/10.1016/j.jhazmat.2014.04.028
13. Marco Tammaro Marco, Valeria Fiandra, … Amedeo Lancia, (2017) Photocatalytic degradation of atenolol in aqueous suspension of new recyclable catalysts based on titanium dioxide, Journal of Environmental Chemical Engineering, Volume 5, Issue 4, Pages 3224-3234 doi.org/10.1016/j.jece.2017.06.026
14. Tay K.S, N.A. Rahman, M.R. Bin Abas, Cha. of atenolol transformation products in ozonation by using rapid resolution high-performance liquid chromatography/quadrupole-time-of-flight mass spectrometry, Microchem. J. 99 (2011) 312-326.
15. Jeirani Z, Niu C.H., Soltan J., (2017) Adsorption of emerging pollutants on activated carbon, Reviews in Chemical Engineering 33 (5), 491-522, 153.
16. Haro, Nathalia & Del Vecchio, Paola & Marcilio, Nilson & Féris, Liliana. (2017). Removal of atenolol by adsorption – Study of kinetics and equilibrium. Journal of Cleaner Production. 154. 214-219. 10.1016/j.jclepro.2017.03.217.
17. Kyzas G.Z, A. Koltsakidou, S.G. Nanaki, D.N. Bikiaris, D.A. Lambropoulou, Removal of beta-blockers from aqueous media by adsorption onto graphene oxide, Sci. Total Environ. 537 (2015) 411–420. DOI: 10.1016/j.scitotenv.2015.07.144
18. Paulchamy B, Arthi G, Lignesh BD (2015) A Simple approach to stepwise synthesis of graphene oxide nanomaterial. J Nanomed Nanotechnology 6:253. doi:10.4172/2157-7439.1000253
19. Píšťková Veronika, Minoo Tasbihi, Milada Vávrová, Urška Lavrenčič Štangar, (2015) Photocatalytic degradation of β-blockers by using immobilized titania/silica on glass slides, Journal of Photochemistry and Photobiology A: Chemistry, Volume 305, Pages 19-28, doi.org/10.1016/j.jphotochem.2015.02.014
20. Hu Jinyuan, Xueping Jing, Li Zhai, Jing Guo, Kun Lu, Liang Mao (2019) BiOCl facilitated photocatalytic degradation of atenolol from water: Reaction kinetics, pathways and products, Chemosphere, Volume 220, Pages 77-85, doi.org/10.1016/j.chemosphere.2018.12.085
21. Kaitano, H.V. and Mudono, S. (2023) Investigating on a Process Method of Beneficiating and Increasing the Graphite Purity to 99% Grade. Journal of

DOI: 10.56892/bima.v9i1A.1236

Analytical Sciences, Methods and Instrumentation, 13, 39-52. doi.org/10.4236/jasmi.2023.134004

22. ACS, Pencils and Erasers (2018), The Secret Science of Stuff, Pg 1-3. www.acs.org/kids
23. Gurzęda, B., Subrati, A., Florczak, P., Kabacińska, Z.,… Krawczyk, P. (2020). Two-step synthesis of well-ordered layered graphite oxide with high oxidation degree. Applied Surface Science, 507, 145049. doi:10.1016/j.apsusc.2019.145049
24. Kiciński Wojciech, Dyjak Sławomir (2020) Transition metal impurities in carbon-based materials: Pitfalls, artifacts and deleterious effects, Carbon, Volume 168, 2020, Pages 748-845, doi:10.1016/j.carbon.2020.06.004
25. Dhakate, S. R., Singh, B. P., Gupta, B. K., Subhedar, K. M., Srivastava, S. K., ... & Ramanujam, J. (2020). Advanced materials for strategic and societal applications. Metrology for inclusive growth of India, 811-879.
26. Sankaran, K. J., & Haenen, K. (2020). Properties of Carbon Bulk Materials: Graphite and Diamond. Synthesis and Applications of Nanocarbons, 1-23.
27. Ali, Z., Yaqoob, S., Yu, J., & D'Amore, A. (2024). Critical Review on the Characterization, Preparation, and Enhanced Mechanical, Thermal, and Electrical Properties of Carbon Nanotubes and Their Hybrid Filler Polymer Composites for Various Applications. Composites Part C: Open Access, 100434. doi.org/10.1016/j.jcomc.2024.100434
28. Kim, S., Saito, M., Wei, Y., Bhuyan., ... & Park, S. (2023). Stretchable and wearable polymeric heaters and strain sensors fabricated using liquid metals. Sensors and Actuators A: Physical, 355, 114317.